Bollettino di Geofisica Teorica ed Applicata Vol. 61, n. 2, pp. 219-232; June 2020
DOI 10.4430/bgta0312

Electrical signatures of a permeable zone in carbonates hosting local geothermal manifestations: insights for the deep fluid flow in the Gargano area (south-eastern Italy)

S. Tripaldi

Dipartimento di Scienze della Terra e Geoambientali, Università degli Studi "Aldo Moro", Bari, Italy

(Received: 11 July 2019; accepted: 11 December 2019)

ABSTRACT In northern Apulia (Italy), geothermal evidence can be associated to structural conditions. The area is characterised by a thick calcareous and dolomitic succession, affected by seismogenic faults and karst dissolution, and by the presence of some surficial geothermal pieces of evidence (coastal springs and well waters). In order to contribute to a better understanding of the deep circulation, an audio-magnetotelluric (AMT) survey was carried out. Soundings were acquired at 22 sites along a 27-km long profile crosscutting the Gargano Promontory and the Tavoliere Plain. A 2D inversion was undertaken providing a resistivity model down to 3 km b.s.l.. In the Tavoliere Plain the resistivity mainly increases with depth. Towards the Gargano area, a low-resistivity layer is interpreted as a fracture network which may favour fluid circulation. The supposed geometry of the permeable zone matches well with the structural interpretation proposed by independent studies. Thus, the present AMT study enabled imaging the first order geological structures that channel deep fluids as locally recognised by boreholes and natural manifestations at the surface.

Key words: audio-magnetotelluric survey, 2D inversion, local geothermal manifestations, fluid pathways.

1. Introduction

In terms of heat flow, Italy is characterised by high values (with local peaks up to 600-1000 mW/m^2) in its western side and, conversely, by low values (around 30-40 mW/m^2) in its eastern side (Della Vedova *et al*., 2001). However, in a few localised sectors of eastern Italy, even in the Mesozoic carbonate platform, heat flow exceeds the average values. This is the case of the Gargano area (NE Apulia), where local thermal springs highlight the phenomenon (Fig. 1).

In geothermal environments, various geophysical methods can be applied in order to contribute to a better understanding of the deep fluid circulation. The magnetotelluric (MT) method is considered one of the most suitable methods because of the relationship between resistivity and geothermal key parameters such as temperature, occurrence of hydrothermal minerals, salinity, and porosity (Ussher *et al*., 2000; Hersir and Árnason, 2009). Moreover, its investigation depth is compatible with the depth of the main targets. Resistivity contrasts between reservoirs and surrounding rocks have for a long time been considered for exploration and resource assessment, especially in high temperature systems. However, several studies testify to the effectiveness of the

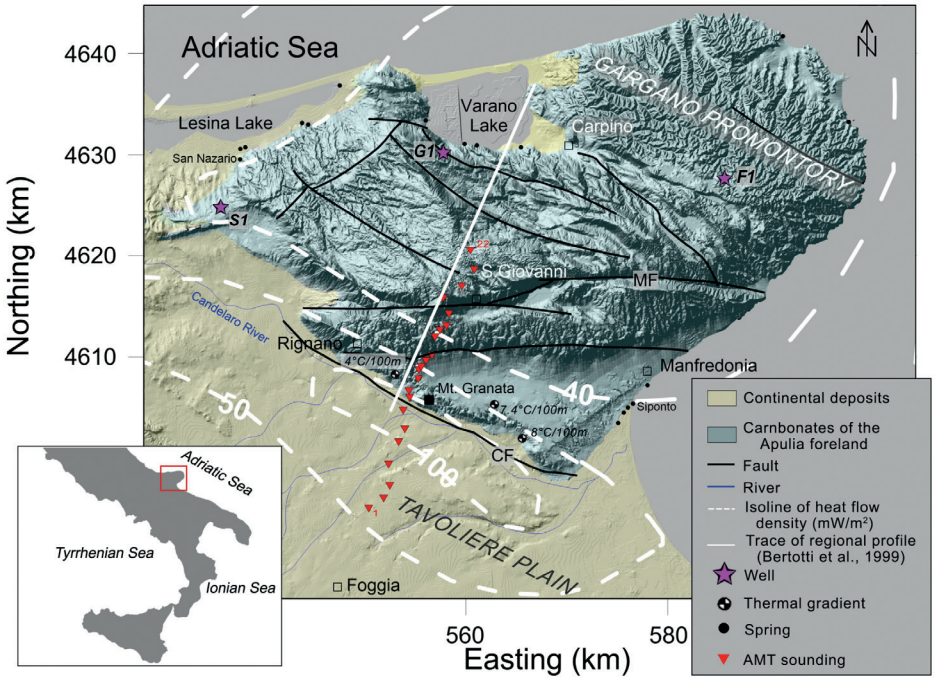

Fig. 1 - Simplified geologic map of the survey area (redrawn after Brankman and Aydin, 2004; Patacca and Scandone, 2004; Spalluto and Pieri, 2008) overlaid on a shaded relief map based on the 20-m digital elevation model from Rete del Sistema Informativo Nazionale Ambientale. Isoline of surface heat flow density (Della Vedova *et al*., 2001) redrawn from The Italian National Geothermal Database. CF: Candelaro Fault; MF: Mattinata Fault.

method even in medium to low enthalpy environments (Arango *et al*., 2009; Muñoz *et al*., 2010; Blake *et al*., 2016; Delhaye *et al*., 2019). Results from borehole and geochemical data support the geological interpretation from the MT resistivity models, thus permitting the development of conceptual models that account for the relationships among geothermal resources, properties of rocks, and geological structures (Cumming, 2009; Siniscalchi *et al*., 2019). Comprehensive reviews can be found in Spichak and Manzella (2009), Flóventz *et al*. (2012), and Muñoz (2014).

This work aims to characterise the geophysical features of the subsoil in the northern Apulia region in a geothermal prospective. Here, calcareous-dolomitic rocks host groundwater with remarkable temperature differences, resulting, at the top of the fractured rock aquifer, from about 14°C (Carpino locality) to 26°C (SE of Monte Granata). Similar differences were also observed in other localities, even among closer sites (Cotecchia and Magri, 1966). This temperature range is regional, since, accordingly, even in numerous coastal springs groundwater outflows at temperatures between 14°C (springs near the Varano Lake) and 27°C (San Nazario spring) (Cotecchia and Magri, 1966). In this context, several studies were carried out in the Gargano area. These highlighted that localised springs outflow geothermal water without temperature changes over time (Cotecchia and Magri, 1966; Cotecchia, 2014), thus accounting for a structural control on fluid pathways.

Several wells were drilled in the Gargano area for oil exploration and were, therefore, located far from the heat flux anomalies. For the aim of this paper, information is scarce and the little coming from seismological, gravity, magnetic, and MT studies is of regional relevance (Speranza and Chiappini, 2002; Patella *et al*., 2005; Tassis *et al*., 2013; Improta *et al*., 2014).

Thus, an image of the substratum to delineate geothermal targets is still lacking. To fill this gap, an audiomagnetotelluric (AMT) investigation, consisting of 22 soundings, was carried out across the Gargano Promontory and the Tavoliere Plain (Fig. 2), crosscutting the main heat flow anomaly of this area (Della Vedova *et al*., 2001). By 2D resistivity modelling, the main geological structures controlling the fluids pathways were imaged.

2. Geological setting

The Apulia region (southern Italy) is part of the present foreland of both the NE-vergent southern Apennines and the SW-vergent Dinarides, both tectonically active during the Neogene (Doglioni *et al*., 1994) and it is dominantly characterised by the Mesozoic platform belonging to the Adria microplate.

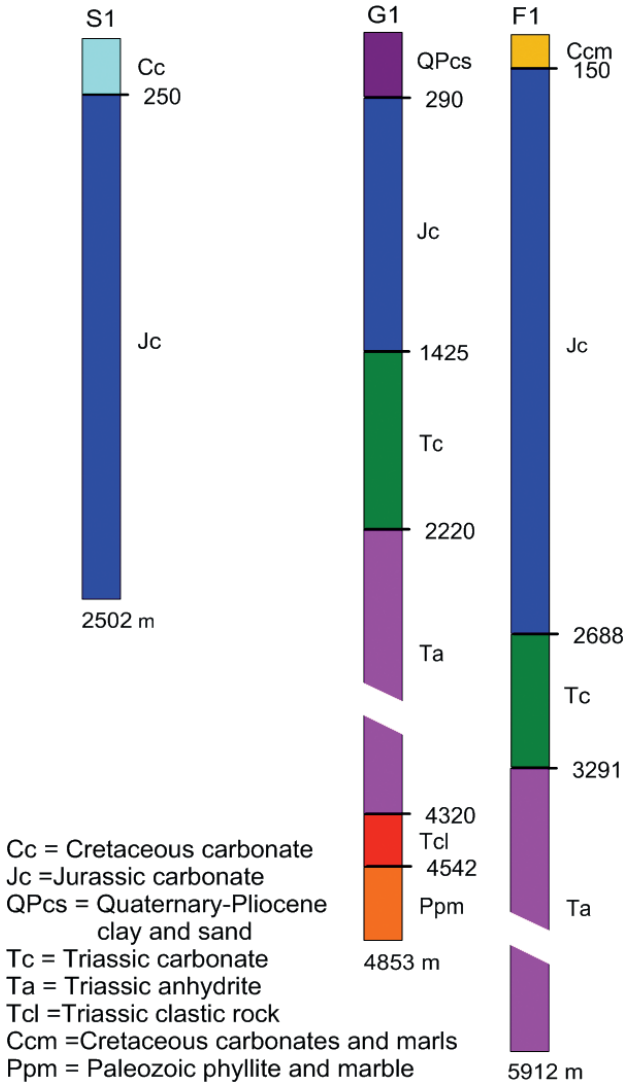

Fig. 2 - Stratigraphic logs from S1 (Sannicandro1), G1 (Gargano 1), and F1 (Foresta Umbra 1) wells redrawn after Zunino *et al*. (2012). The location of the S1, G1, F1 wells is shown in Fig. 1.

In the Gargano area, the stratigraphic succession is known from well logs; the three boreholes in the surroundings of the AMT prospections (Figs. 1 and 2) highlight rocks from Permian to Cretaceous, these latter overlain by Pliocene-Quaternary sediments (Fig. 2). The thickness of the Triassic evaporitic rocks can reach more than 2 km and that of the Mesozoic carbonatic succession reaches more than 3 km. Detailed descriptions on the stratigraphic sequences can be found in Bosellini *et al*. (1999), Bosellini and Morsilli (2001), and Patacca *et al*. (2008).

This succession was involved in the Apennines deformation (Finetti, 1982; Ortolani and Pagliuca, 1989; Funiciello *et al*., 1991; Billi *et al*., 2007). For this study, the most prominent structures are those developed in the brittle regime, determining E-W, ENE-WSW, and NW-SE striking fault zones (Brankman and Aydin, 2004; Spalluto and Pieri, 2008). Their kinematics is still debated, although strike-slip and normal components are considered dominant. In this framework, the most significant geological structure is considered the Mattinata Fault (Fig. 1, Salvini *et al*., 1999; Patacca and Scandone, 2004), a sub-vertical almost E-W striking fault that entirely cuts the Gargano Promontory. According to Bertotti *et al*. (1999), the Gargano underwent deformation in a compressive regime during the Neogene. This evolution determined a regional back-thrust of which the detachment level could be located in the evaporitic level (Fig. 3). In this view, the previously described fault system is comprised in the hanging wall.

The hydrogeological knowledge derives mostly from the extensive work of Cotecchia and Magri (1966), revised and updated in the light of recent studies (Cotecchia, 2014), briefly summarised in the following. The surface drainage network is related to the ground permeability, karst evolution processes, and tectonic structures. Perennial watercourses are absent in the central-western area of the Gargano Promontory. Torrential waters flow in the wide and deep morphological depressions from where local high permeable rock volumes favour infiltration down to depth. According to Cotecchia (2014), the main water resource is contained in a vast deep fractured carbonate aquifer with the base at sea level. By this, interfingering relations between meteoric and marine waters are frequent close to the coastal areas. Borehole logs indicate that the groundwater circulates from 650 to 800 m b.g.l. within carbonates, where flowing is enhanced by the typical karst features like joints and cavities (Zezza *et al*., 1996). Fault and damage zones are considered preferential groundwater paths, influencing the location and distribution of coastal springs (Grassi and Tadolini, 1991).

The Tavoliere Plain is bordered by the Candelaro River (Fig.1). Its course is believed to coincide with a regional fault zone, the Candelaro Fault (Salvini *et al*., 1999 and references

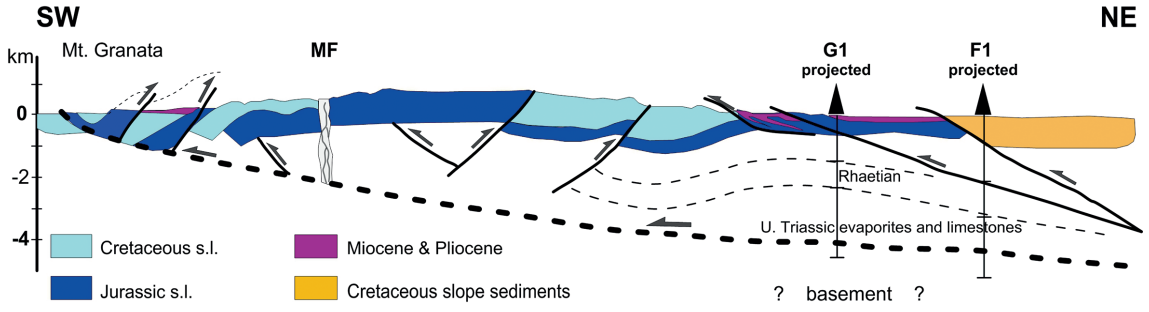

Fig. 3 - Geological section of the Gargano area redrawn after Bertotti *et al*. (1999). The trace of the cross section is shown in Fig. 1.

therein). The plain is characterised by the presence of a surficial watercourse network constituted by the Candelaro River and its tributaries. The groundwater circulation is influenced by the texture of the alluvial sediments, determining differences in porosity and permeability (Caldara and Pennetta, 1993; Maggiore *et al*., 1996). However, the hydro-isopiezes distribution indicates that the Gargano and Tavoliere aquifers are almost parallel to the Candelaro Fault, thus indicating that groundwater converges towards the fault zone and farther SE flowing towards the sea (Cotecchia and Magri, 1966). Near the Candelaro Fault, a thermal gradient ranging from 4°C/100 m to 8°C/100 m was observed by water temperature measurements in three shallow (100 m deep) wells (Cotecchia and Magri, 1966, Fig. 1). The corresponding heat flow values, ranging from 113 to 142 mW/m^2, were estimated by Mongelli and Ricchetti (1970). The same authors speculated that this heat flow anomaly may be ascribed either to regional (Moho discontinuity rising) or to local causes. According to Maggiore and Pagliarulo (2004), the thermal anomalies originate from the rising of deep warm water along fractures. Recently, Filippucci *et al*. (2019b) related the depth of earthquakes to the surface heat flow density by using a thermo-rheological model. Their results suggest that the brittle/ductile transition depth is at about 7 km depth in the Candelaro area and at about 24 km in the Gargano Promontory (Fig. 1).

3. AMT data and analysis

The MT method exploits natural electromagnetic fields to determine the electrical resistivity of the subsurface (Tikhonov, 1950; Cagniard, 1953). In the frequency domain, under the plane wave assumption, the complex MT impedance tensor Z relates the horizontal components of the electric (E) and magnetic (H) fields:

$$\begin{bmatrix} E_x(\omega) \\ E_y(\omega) \end{bmatrix} = \begin{bmatrix} Z_{xx}(\omega) & Z_{xy}(\omega) \\ Z_{yx}(\omega) & Z_{yy}(\omega) \end{bmatrix} \begin{bmatrix} H_x(\omega) \\ H_y(\omega) \end{bmatrix} \quad (1)$$

Routinely, apparent resistivities (Eq. 2) and phases (Eq. 3) are obtained from the elements of Z:

$$\rho_{ij}^{a}(\omega) = \frac{1}{\mu_0 \omega} \left| Z_{ij}(\omega) \right|^2 \quad (2)$$

$$\phi_{ij}(\omega) = tan^{-1} \left[\frac{Im(Z_{ij}(\omega))}{Re(Z_{ij}(\omega))} \right] \quad (3)$$

where ω is the angular frequency and μ_0 is the free space magnetic permeability.

Typical broadband MT surveys, 10^{-3}-10^{3} Hz (Chave and Jones, 2012), allow subsurface investigation depths ranging from a few hundred metres to kilometres. For shallower and detailed investigation purposes, recordings in the higher frequency band (10-10^5 Hz) are needed, thus implying AMT investigations.

In this work, an AMT survey was carried out with a Stratagem EH4 system performing 22 soundings along an approximately 27 km profile. The interdistance between the sounding sites varies from ~500 to ~2400 m. Two orthogonal components of electric field and two orthogonal

components of magnetic field were recorded in the N-S and E-W frame. For each site a different set of magnetic and electric sensors was used; BF-6 induction coils and steel electrodes were used to respectively measure the horizontal components of the magnetic and the electric fields in the frequency range from 10 Hz to 100 kHz. BF-10 induction coils and unpolarisable $Cu/CuSO_4$ electrodes were used to record the data in the frequency range 0.1-10.0 Hz. A controlled source was also employed to strengthen the signal in the AMT dead band [1-5 kHz (García and Jones, 2002)]. For each frequency sub-band, time series were processed using the Geometrics Image software. To reduce noise in the data, time series were inspected rejecting suspicious segments prior to the cross-power calculations. A coherence threshold of 0.85 for electric and magnetic fields was used to get impedance estimations.

Data quality control was performed by inspecting apparent resistivity and phase curve trends along with their consistency. Most of the curves seem reliable, being characterised by a smooth trend, although some data indicate inferior quality in correspondence of the AMT and MT dead band (Fig. 4). As for the former, the use of the controlled source was not always effective. A splitting of the xy and yx curves is observed for several soundings carried out in the central and northern part of the profile, suggesting the presence of 2D (or 3D) resistivity structures.

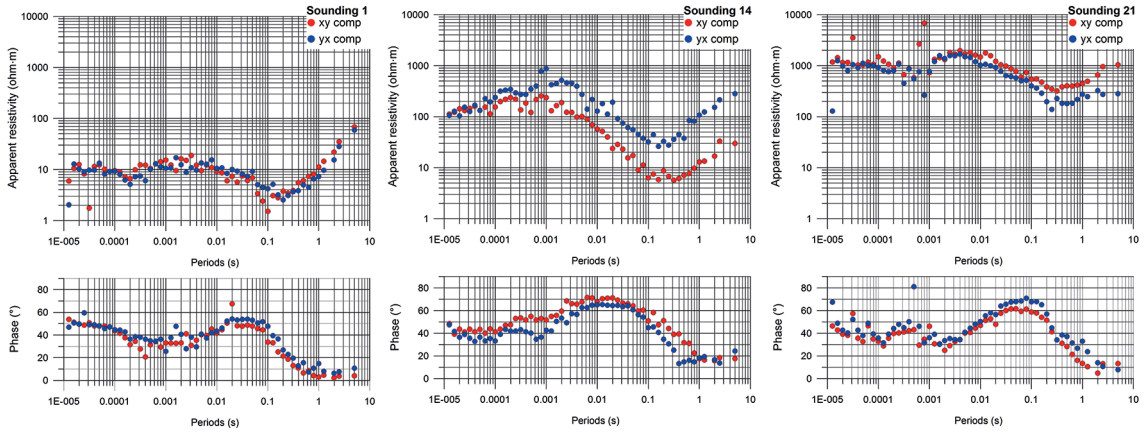

Fig. 4 - Apparent resistivity and phase curves shown in original form before rotation. Sounding 1 is the southernmost site along profile (Fig. 1).

At the shorter periods (shallower depths), the curves show a systematic increase in apparent resistivity values (from 10 to 1000 ohm×m) northwards along the profile (Fig. 4). These values are in accordance with the geologic framework of the sites. Indeed, very low values (10 ohm×m) characterise all sites located in the Tavoliere Plain, where alluvial deposits outcrop. Further to the north, all curves report values from 100 up to 1000 ohm×m consistently with the increasing presence of limestone outcrops. The frequency-dependent attenuation of the electromagnetic field implies a minor penetration depth in the more conductive southern area with respect to the northern one.

Dimensionality and directionality of the geoelectrical structures were investigated following the approach of Weaver *et al*. (2000), which involves a set of independent parameters that are rotational invariants of the MT impedance tensor. 1D and 2D dimensionality cases are recognised

by the annulment of some of the seven invariants. Since impedance estimates are affected by errors, which in turn propagate on the related invariants, threshold values were considered as suggested by Martí *et al*. (2004). A different degree of complexity is revealed depending both on the position of the soundings and on the considered periods (Fig. 5). For periods shorter than 5×10^{-3} s 1D, 2D and 3D cases are present, but 1D cases mainly occur for soundings located in the south-western area (soundings 1-7). For periods longer than 5×10^{-3} s, a 2D behaviour represents the majority of cases even if indeterminate cases are observed for soundings located in the south-western area, while 3D cases mostly manifest for soundings in the north-eastern area. Summarising, a 1D-2D scenario may be assumed for the south-western area and a 2D-3D scenario for the north-eastern one. Impedance strike angle was estimated for each sounding at each period when data dimensionality satisfies the 2D assumption. However, since the choice of the cut-off value is somewhat arbitrary (Weaver *et al*., 2006), strike angle was calculated also for 3D cases within 2D case ranges. Fig. 5 shows two rose diagrams of strike directions estimated for two period ranges. The strike values in the shorter period range (<0.003 s) are more dispersed than those in the longer one (>0.003 s). Thus, a well defined geoelectric strike is not detectable in the shortest period range, perhaps because of the dominant one-dimensional nature of the resistivity

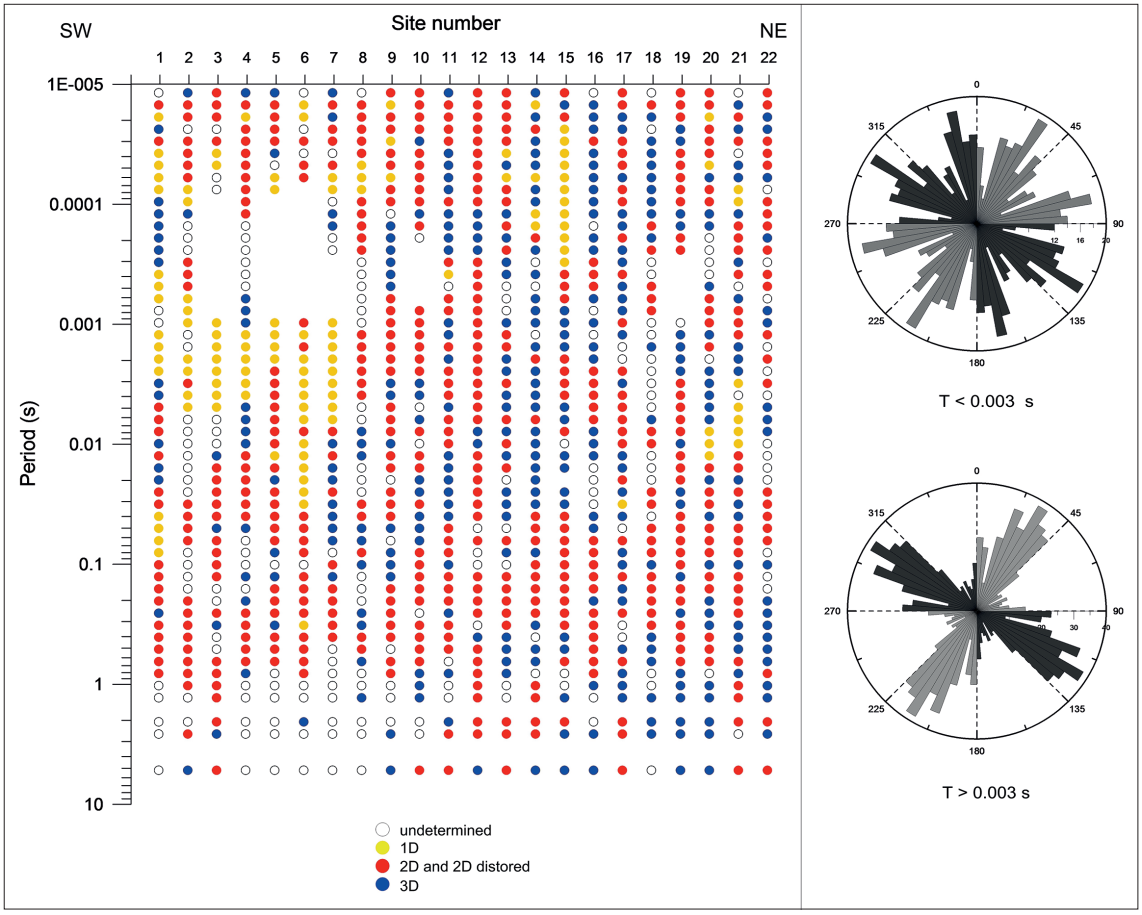

Fig. 5 - Left panel: result of data dimensionality analysis. Right panel: upper and lower rose diagrams for the periods lower and higher than 0.003 s, respectively.

structure or because of the higher level of noise. In the longer period range, a strike direction value ranging between N45°W and N70°W, with an inherent 90° ambiguity, is found. The estimated strike is almost consistent with the direction of the numerous mapped faults, which are NW-SE and WNW-ESE oriented (e.g. Brankman and Aydin, 2004). It should be noted that a minor cluster, which indicates W-E oriented structures, is also observed. According to this result, using the procedure described in Weaver *et al*. (2000), data were corrected for shallow (shorter periods) distortions and rotated by N20°E, which was considered the best compromise to represent the regional structures (longer periods).

The generated TE (currents flowing parallel to the strike direction) and TM (currents flowing perpendicular to the strike direction) mode responses were inverted using the nonlinear conjugate 2D inversion algorithm of Rodi and Mackie (2001). Since no independent data were available, static shift effects (Pellerin and Hohmann, 1990; Tripaldi *et al*., 2010; Delhaye *et al*., 2017) could not be removed. To resolve the issue and to evaluate primary structures retrieved by the observed data, several inversions, with different parameter settings, were run.

The presented resistivity model was obtained using a homogeneous starting model (100 ohm×m) including topography. The regularisation parameter (τ) was chosen considering the trade-off between data fitting and model roughness, according to the L-curve, and was set to 10. For the TM apparent resistivity and phase data, the error floor was set to 10 and 5%, respectively; as for the TE mode resistivity and phase, error floor was set to 30 and 5%, respectively. These settings were preferred since a greater weight to the phase data can minimise effects of static shift. Notably, the TE apparent resistivity was down weighted since it is more susceptible to 3D effects (Tauber *et al*., 2003; Becken *et al*., 2008a; Becken *et al*., 2008b). An acceptable normalised root-mean-square (nRMS) misfit value of 2.2 was obtained. Fig. 6 shows the apparent resistivity and

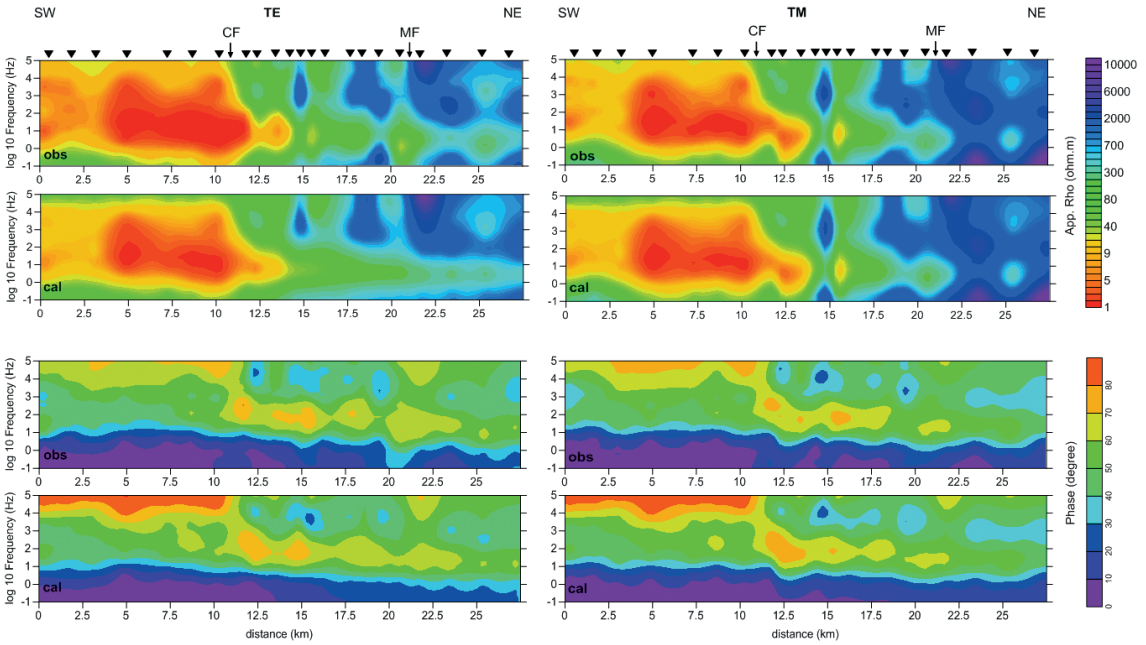

Fig. 6 - Pseudosections of the observed (obs) and calculated (cal) data along the AMT profile. CF: Candelaro Fault; MF: Mattinata Fault.

phase pseudosections of the observed and modelled data. As shown, the fit is generally good except for the highest frequency range of soundings characterised by the lowest resistivity values. Despite the difficulty in fitting these data, the model satisfactorily reproduces the observed wide resistivity variations, hence it recovers the primary electrical signatures which are the main target of the present work.

4. Results and discussion

The model images resistivity values varying over a wide range (1-10 ohm×m; Fig. 7). Consistently with the results from the dimensionality analysis (Fig. 5), the electrical signature is more complex in the north-eastern portion of the model with respect to the one highlighted in the south-western part. For sake of clarity, these two different zones will first be discussed separately and then together.

From the south-westernmost edge of the model to the Candelaro Fault (Fig. 7), a shallow conductive layer (resistivity values <40 ohm×m) is confined in the first ~ 500 m of depth. Within this layer, the lowest resistivity values (<10 ohm×m) correspond to the area where the maximum heat flow anomaly (100 mW/m^2) is recorded (Della Vedova *et al*., 2001; Fig. 1). This shallow conductive layer gently deeps towards SW, overlying a resistive bedrock.

This resistivity pattern can be explained considering the stratigraphic succession and the hydrological information from the study area. In fact, the Quaternary clayey and inter-bedded sandy sediments, overlying the carbonate bedrock, host a multi-layered aquifer-aquitard system (Maggiore *et al*., 1996) where electrical-conductivity measurements indicate values up to 2500 microS/cm (Masciale *et al*., 2011). Thus, the occurrence of aquifers, brackish water levels, numerous surficial water courses and the high cation exchange capacity of clay minerals, all concur to the bulky conductivity enhancement of the shallower level (Fig. 7). Contrastingly, the high resistivity bedrock can be ascribed to the Jurassic-Cretaceous carbonate undeformed platform.

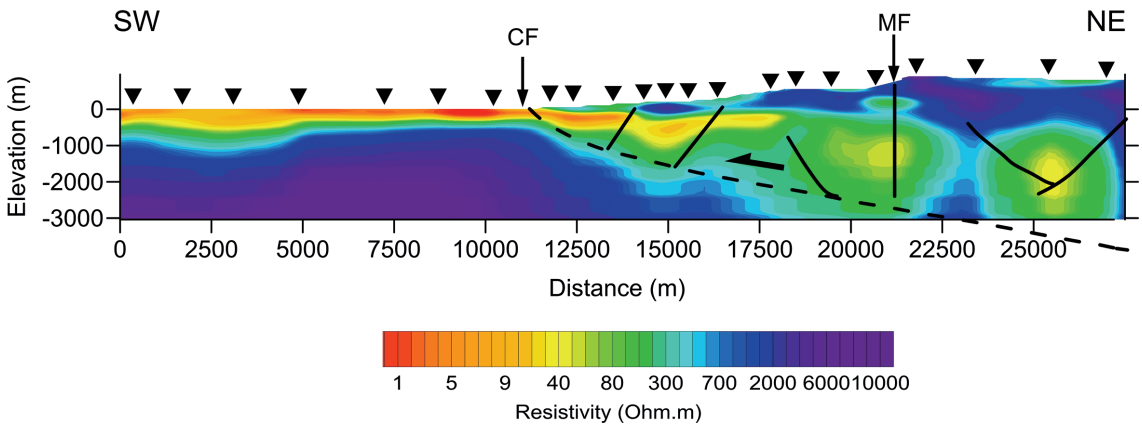

Fig. 7 - Resistivity model. Overlaid structural features are redrawn after Bertotti *et al*. (1999). CF: Candelaro Fault; MF: Mattinata Fault.

Notwithstanding the good correlation with available geological and hydrogeological data, the quasi 1D electrical signature is difficult to interpret in terms of geothermal targets. However, it should be stressed that shallow and high-conductivity layers may limit the AMT resolution at depth, masking targets of interest. Within sedimentary contexts, this issue, i.e. the blanketing of deep features, can be addressed acquiring data with a denser site spacing (Muñoz *et al*., 2010).

As a simplified picture, the north-eastern portion of the model (from the Candelaro Fault to the north-eastern end of the profile; Fig. 7) is constituted by a resistive background hosting conductive and moderately conductive anomalies dipping NE-wards. The shallow resistive cover is explained by the outcropping carbonates rocks. A shallow resistivity lowering corresponds to the Mattinata Fault zone (Fig. 7) and is connected to a deep-rooted conductive body. Several studies described the Mattinata Fault as a the sub-vertical fault zone (Patacca and Scandone, 2004). The present AMT resolution does not permit a detailed image of the fault zone, especially regarding its damage zone width. The recovered electrical feature may derive from a bulky conductive body locally affected by partitioned deformation.

At about 10 km to the northern end of the profile, the stratigraphic borehole log (G1 in Fig. 1) reports, from the top to the bottom, carbonate rocks down to 2220 m b.g.l. and an evaporite level down to 4320 m b.g.l. These rock units, depending on their own sedimentary and tectonic evolution, can exhibit variable petro-physical properties, influencing permeability and fluid flow: geological bodies with low porosity and permeability are characterised by high resistivity values; on the contrary, secondary permeability can lead to huge resistivity decreases (Schön, 2004). These considerations suggest that the NE-ward conductive dipping level could be associated to a fractured water bearing unit, although its lithological composition and/or textural homogeneity are unknown. At greater depth, below the NE-dipping conductive level, the resistivity increases indicating an undeformed, or less deformed, lithological level. This evidence suggests that the conductive level is the consequence of localised deformation, such as a brittle shear zone. This interpretation agrees with the structural reconstruction proposed by Bertotti *et al*. (1999), here reported in Fig. 3.

The entire model displays a sharp change of resistivity both in its shallow and deep part, clearly visible at the termination of the shear zone. This variation corresponds at the surface with the Candelaro Fault zone, where a sharp decrease of the heat flow is measured, thus implying a steep gradient dipping to NE-wards (Fig. 1). Furthermore, in this area, shallow seismic events (0-5 km deep) are clustered (de Lorenzo *et al*., 2017; Filippucci *et al*., 2019b) and a positive coda attenuation (Q_c) anomaly is retrieved (Filippucci *et al*., 2019a). Many MT crustal studies (Aizawa *et al*., 2017 and references herein) report that earthquakes occur in resistive-conductive transition zones. When available, the combined analysis of electrical anomalies and seismicity patterns may reveal the occurrence of fluid-assisted active fault zones (Bedrosian *et al*., 2004; Aizawa *et al*., 2017). Here, the above mentioned seismological observations along with the abrupt change in resistivity (transition zone) may represent differences in the elastic properties, separating the southern compact basement from the fractured weaker rocks hosting fluids. This scenario, suggesting circulation of deep fluids, is also supported by the anomalous values of Rn, 3He/4He, and Hg measured in the Montegranata well, in proximity of the Candelaro Fault (Salvi *et al*., 1999).

5. Conclusions

This paper reports the first results of an AMT survey performed in northern Apulia, Italy. The 2D model envisages a fairly simple resistivity distribution, approximately 1D towards SW, while the juxtaposition of different resistivity units characterises the north-eastern portion of the model. The most striking result concerns the detection of the NE dipping conductive layer which connects the surficial conductive layer, recognised to the SW of the Candelaro Fault, with the low resistivity sector interbedded between two high to moderate resistivity units. Thus, this resistivity model suggests the occurrence of a permeable corridor dipping to the NE, possibly determined by deformational events occurring during the Miocene-Pliocene shortening (Bertotti *et al*., 1999). This permeable zone is then affected by more recent structures, such as the Mattinata Fault zone. These faults can reasonably increase the permeability determining a good hydraulic conductivity, favouring groundwater circulation and the upflow of deep heated fluids in correspondence of the Candelaro Fault area. Finally, the present AMT survey shed light on the main resistivity units, allowing a preliminary geological interpretation. However, future broadband MT data acquisitions are desirable to better constrain the geometry of the geological structures and the permeable levels at depth.

Acknowledgements. This work was supported by "Intervento cofinanziato dal Fondo di Sviluppo e Coesione 2007-2013 - APQ Ricerca Regione Puglia, Programma regionale a sostegno della specializzazione intelligente e della sostenibilità sociale ed ambientale - Future In Research". I wish to thank Gerardo Romano and Agata Siniscalchi for encouraging this work and for data acquisition. I wish to thank Domenico Liotta for constructive discussions. Thanks are also due to two anonymous reviewers for their helpful comments and suggestions, which helped improve the manuscript.

REFERENCES

Aizawa K., Asaue H., Koike K., Takakura S., Utsugi M., Inoue H., Yoshimura R., Yamazaki K., Komatsu S., Uyeshima M., Koyama T., Kanda W., Shiotani T., Matsushima N., Hata M., Yoshinaga T., Uchida K., Tsukashima Y., Shito A., Fujita S., Wakabayashi A., Tsukamoto K., Matsushima T., Miyazaki M., Kondo K., Takashima K., Hashimoto T., Tamura M., Matsumoto S., Yamashita Y., Nakamoto M. and Shimizu H.; 2017: *Seismicity controlled by resistivity structure: the 2016 Kumamoto earthquakes, Kyushu Island, Japan*. Earth Planets Space, **69**, 4, doi: 10.1186/s40623-016-0590-2.

Arango C., Marcuello A., Ledo J. and Queralt P.; 2009: *3D magnetotelluric characterization of the geothermal anomaly in the Llucmajor aquifer system (Majorca, Spain)*. J. Appl. Geophys., **68**, 479-488, doi: 10.1016/j.jappgeo.2008.05.006.

Becken M., Ritter O. and Burkhardt H.; 2008a: *Mode separation of magnetotelluric responses in three-dimensional environments*. Geophys. J. Int., **172**, 67-86, doi: 10.1111/j.1365-246X.2007.03612.x.

Becken M., Ritter O., Park S.K., Bedrosian P.A., Weckmann U. and Weber M.; 2008b: *A deep crustal fluid channel into the San Andreas Fault system near Parkfield, California*. Geophys. J. Int., **173**, 718-732, doi: 10.1111/j.1365-246X.2008.03754.x.

Bedrosian P.A., Unsworth M.J., Egbert G.D. and Thurber C.H.; 2004: *Geophysical images of the creeping San Andreas Fault: implications for the role of crustal fluids in the earthquake process*. Tectonophys., **385**, 137-158, doi: 10.1016/j.tecto.2004.02.010.

Bertotti G., Casolari E. and Picotti V.; 1999: *The Gargano Promontory: a Neogene contractional belt within the Adriatic Plate*. Terra Nova, **11**, 168-173.

Billi A., Gambini R., Nicolai C. and Storti F.; 2007: *Neogene-Quaternary intraforeland transpression along a Mesozoic platform-basin margin: the Gargano Fault system, Adria, Italy*. Geosphere, **3**, 1-15, doi: 10.1130/GES00057.1.

Blake S., Henry T., Muller M.R., Jones A.G., Moore J.P., Murray J., Campanyà J., Vozar J., Walsh J. and Rath V.; 2016: *Understanding hydrothermal circulation patterns at a low-enthalpy thermal spring using audio-magnetotelluric data: a case study from Ireland*. J. Appl. Geophys., **132**, 1-16, doi: 10.1016/j.jappgeo.2016.06.007.

Bosellini A. and Morsilli M.; 2001: *Il Promontorio del Gargano cenni di geologia e itinerari geologici*. In: Grenzi C. (ed), Quaderni del Parco Nazionale del Gargano, Foggia, Italy, pp. 1-48.

Bosellini A., Morsilli M. and Neri C.; 1999: *Longterm event stratigraphy of the Apulia Platform margin (Upper Jurassic to Eocene, Gargano, southern Italy)*. J. Sediment. Res., **69**, 1241-1252, doi: 10.2110/jsr.69.1241.

Brankman C. and Aydin A.; 2004: *Uplift and contractional deformation along a segmented strike-slip fault system: the Gargano Promontory, southern Italy*. J. Struct. Geol., **26**, 807-824, doi: 10.1016/j.jsg.2003.08.018.

Cagniard L.; 1953: *Basic theory of the magnetotelluric method of geophysical prospecting*. Geophys., **18**, 605-645.

Caldara M. and Pennetta L.; 1993: *Nuovi dati per la conoscenza geologica e morfologica del Tavoliere di Puglia*. Bonifica, **3**, 25-42.

Chave A.D. and Jones A.G. (eds); 2012: *The magnetotelluric method: theory and practice*. Cambridge University Press, New York, NY, USA, 584 pp., doi: 10.1017/CBO9781139020138.

Cotecchia V.; 2014: *Le acque sotterranee e l'intrusione marina in Puglia: dalla ricerca all'emergenza nella salvaguardia della risorsa*. Mem. Descr. Carta Geologica d'Italia, **XCII**, 15-660.

Cotecchia V. and Magri G.; 1966: *Idrogeologia del Gargano*. Geol. Appl. e Idrogeol., **1**, 1-80.

Cumming W.; 2009: *Geothermal resource conceptual models using surface exploration data*. In: Proc., 34th Workshop on Geothermal Reservoir Engineering, Stanford University, Stanford, CA, USA, 6 pp.

de Lorenzo S., Michele M., Emolo A. and Tallarico A.; 2017: *A 1D P-wave velocity model of the Gargano Promontory (southeastern Italy)*. J. Seismolog., **21**, 909-919, doi: 10.1007/s10950-017-9643-7.

Delhaye R., Rath V., Jones A.G., Muller M.R. and Reay D.; 2017: *Correcting for static shift of magnetotelluric data with airborne electromagnetic measurements: a case study from Rathlin Basin, northern Ireland*. Solid Earth, **8**, 637-660, doi: 10.5194/se-8-637-2017.

Delhaye R., Rath V., Jones A.G., Muller M.R. and Reay D.; 2019: *Quantitative geothermal interpretation of electrical resistivity models of the Rathlin Basin, northern Ireland*. Geothermics, **77**, 175-187, doi: 10.1016/j.geothermics.2018.09.012.

Della Vedova B., Bellani S., Pellis G. and Arci P.; 2001: *Deep temperatures and surface heat flow distribution*. In: Vai G.B. and Martini P. (eds), Anatomy of an Orogen: the Apennines and adjacent Mediterranean Basins, Kluwer Academic Publishers, Dordrecht, The Netherlands, Chapter 7, pp. 65-76.

Doglioni C., Mongelli F. and Pieri P.; 1994: *The Puglia uplift (SE Italy): an anomaly in the foreland of the Apenninic subduction due to buckling of a thick continental lithosphere*. Tectonics, **13**, 1309-1321.

Filippucci M., Del Pezzo E., de Lorenzo S. and Tallarico A.; 2019a: *2D kernel-based imaging of coda-Q space variations in the Gargano Promontory (southern Italy)*. Phys. Earth Planet. Inter., **297**, 106313, doi: 10.1016/j.pepi.2019.106313.

Filippucci M., Tallarico A., Dragoni M. and de Lorenzo S.; 2019b: *Relationship between depth of seismicity and heat flow: the case of the Gargano Area (Italy)*. Pure Appl. Geophys., **176**, 2383-2394, doi: 10.1007/s00024-019-02107-5.

Finetti I.; 1982: *Structure, stratigraphy and evolution of central Mediterranean*. Boll. Geof. Teor. Appl., **24**, 247-277.

Flóvenz Ó.G., Hersir G.P., Sæmundsson K., Ármannsson H. and Friðriksson Þ.; 2012: *Geothermal energy exploration techniques*. Compr. Renew. Energy, **7**, 51-95, doi: 10.1016/B978-0-08-087872-0.00705-8.

Funiciello R., Montone P., Parotto M., Salvini F. and Tozzi M.; 1991: *Geodynamical evolution of an intra-orogenic foreland: the Apulia case history (Italy)*. Boll. Soc. Geol. Ital., **110**, 419-425.

García X. and Jones A.G.; 2002: *Atmospheric sources for audio-magnetotelluric (AMT) sounding*. Geophys., **67**, 448-458, doi: 10.1190/1.1468604.

Grassi D. and Tadolini T.; 1991: *La circolazione idrica sotterranea nell'ammasso carbonatico mesozoico del Gargano*. In: Atti, Convegno Ricerca e Protezione delle Risorse Idriche Sotterrenee nelle aree montuose, Brescia, Italy, pp. 333-374.

Hersir G.P. and Árnason K.; 2009: *Resistivity of rocks*. In: Short Course on Surface Exploration for Geothermal Resources, UNU-GTP and LaGeo, Ahuachapan and Santa Tecla, El Salvador, 8 pp.

Improta L., De Gori P. and Chiarabba C.; 2014: *New insights into crustal structure, Cenozoic magmatism, CO_2 degassing, and seismogenesis in the southern Apennines and Irpinia region from local earthquake tomography*. J. Geophys. Res. Solid Earth, **119**, 8283-8311, doi: 10.1002/2013JB010890.

Maggiore M. and Pagliarulo P.; 2004: *Circolazione idrica ed equilibri idrogeologici negli acquiferi della Puglia*. Geologi e Territorio, Periodico dell'Ordine dei Geologi della Puglia, **1 Supplemento**, 13-35.

Maggiore M., Nuovo G. and Pagliarulo P.; 1996: *Caratteristiche idrogeologiche e principali differenze idrochimiche delle falde sotterranee del Tavoliere di Puglia*. Mem. Soc. Geol. Ital., **51**, 669-684.

Martí A., Queralt P. and Roca E.; 2004: *Geoelectric dimensionality in complex geologic areas: application to the Spanish Betic Chain*. Geophys. J. Int., **157**, 961-974, doi: 10.1111/j.1365-246X.2004.02273.x.

Masciale R., Barca E. and Passarella G.; 2011: *A methodology for rapid assessment of the environmental status of the shallow aquifer of "Tavoliere di Puglia" (southern Italy)*. Environ. Monit. Assess., **177**, 245-261, doi: 10.1007/s10661-010-1631-0.

Mongelli F. and Ricchetti G.; 1970: *Heat flow along the Candelaro Fault - Gargano Headland (Italy)*. Geothermics, **2**, 450-458.

Muñoz G.; 2014: *Exploring for geothermal resources with electromagnetic methods*. Surv. Geophys., **35**, 101-122, doi: 10.1007/s10712-013-9236-0.

Muñoz G., Ritter O. and Moeck I.; 2010: *A target-oriented magnetotelluric inversion approach for characterizing the low enthalpy Groß Schönebeck geothermal reservoir*. Geophys. J. Int., **183**, 1199-1215.

Ortolani F. and Pagliuca S.; 1989: *Tettonica transpressiva nel Gargano e rapporti con le catene Appenninica e Dinarica*. Mem. Soc. Geol. Ital., **38**, 205-224.

Patacca E. and Scandone P.; 2004: *The 1627 Gargano earthquake (southern Italy): identification and characterization of the causative fault*. J. Seismolog., **8**, 259-273, doi: 10.1023/B:JOSE.0000021393.77543.1e.

Patacca E., Scandone P., Di Luzio E., Cavinato G.P. and Parotto M.; 2008: *Structural architecture of the central Apennines: interpretation of the CROP 11 seismic profile from the Adriatic coast to the orographic divide*. Tectonics, **27**, TC3006, doi: 10.1029/2005TC001917.

Patella D., Petrillo Z., Siniscalchi A., Impronta L. and Di Fiore B.; 2005: *Magnetotelluric profiling along the CROP-04 section in the southern Appennines*. In: Finetti I. (ed), CROP PROJECT, Deep Seismic Exploration of the central Mediterranean and Italy, Chapter 13, pp. 263-280.

Pellerin L. and Hohmann G.W.; 1990: *Transient electromagnetic inversion: a remedy for magnetotelluric static shifts*. Geophys., **55**, 1242-1250, doi: 10.1190/1.1442940.

Rodi W.L. and Mackie R.L.; 2001: *Nonlinear conjugate gradients algorithm for 2D magnetotelluric inversion*. Geophys., **66**, 174-187, doi: 10.1190/1.1444893.

Salvi S., Quattrocchi F., Brunori C.A., Doumaz F., Angelone M., Billi A., Buongiorno F., Funiciello R., Guerra M., Mele G., Pizzino L. and Salvini F.; 1999: *A multidisciplinary approach to earthquake research: implementation of a Geochemical Geographic Information System for the Gargano Site, southern Italy*. Nat. Hazards, **20**, 255-278.

Salvini F., Billi A. and Wise D.U.; 1999: *Strike-slip fault-propagation cleavage in carbonate rocks: the Mattinata Fault zone, southern Apennines, Italy*. J. Struct. Geol., **21**, 1731-1749, doi: 10.1016/S0191-8141(99)00120-0.

Schön J.H.; 2004: *Physical properties of rocks: fundamentals and principles of petrophysics, 1st ed*. Pergamon, Amsterdam, The Netherlands, 600 pp.

Siniscalchi A., Tripaldi S., Romano G., Chiodini G., Improta L., Petrillo Z., D'Auria L., Caliro S. and Avino R.; 2019: *Reservoir structure and hydraulic properties of the Campi Flegrei geothermal system inferred by audiomagnetotelluric, geochemical, and seismicity study*. J. Geophys. Res. Solid Earth, **124**, 5336-5356, doi: 10.1029/2018JB016514.

Spalluto L. and Pieri P.; 2008: *Carta geologica delle unità carbonatiche mesozoiche e cenozoiche del Gargano sud-occidentale: nuovi vincoli stratigrafici per l'evoluzione tettonica dell'area*. Mem. Descr. Carta Geologica d'Italia, **LXXVII**, 147-176.

Speranza F. and Chiappini M.; 2002: *Thick-skinned tectonics in the external Apennines, Italy: new evidence from magnetic anomaly analysis*. J. Geophys. Res., **107**, 2290, doi: 10.1029/2000JB000027.

Spichak V. and Manzella A.; 2009: *Electromagnetic sounding of geothermal zones*. J. Appl. Geophys., **68**, 459-478, doi: 10.1016/j.jappgeo.2008.05.007.

Tassis G.A., Grigoriadis V.N., Tziavos I.N., Tsokas G.N., Papazachos C.B. and Vasiljević I.; 2013: *A new Bouguer gravity anomaly field for the Adriatic Sea and its application for the study of the crustal and upper mantle structure*. J. Geodyn., **66**, 38-52, doi: 10.1016/j.jog.2012.12.006.

Tauber S., Banks R., Ritter O. and Weckmann U.; 2003: *A high-resolution magnetotelluric survey of the Iapetus suture zone in southwest Scotland*. Geophys. J. Int., **153**, 548-568, doi: 10.1046/j.1365-246X.2003.01912.

Tikhonov A.N.; 1950: *Determination of the electrical characteristics of the deep strata of the Earth's crust*. Dokl. Acad. Nauk., **73**, 295-297.

Tripaldi S., Siniscalchi A. and Spitzer K.; 2010: *A method to determine the magnetotelluric static shift from DC resistivity measurements in practice*. Geophys., **75**, F23-F32, doi: 10.1190/1.3280290.

Ussher G., Harvey C., Johnstone R. and Anderson E.; 2000: *Understanding the resistivities observed in geothermal systems*. In: Proc., World Geothermal Congress 2000, Kyushu Tohoku, Japan, pp. 1915-1920.

Weaver J.T., Agarwal A.K. and Lilley F.E.M.; 2000: *Characterisation of the magnetotelluric tensor in terms of its invariants*. Geophys. J. Int., **141**, 321-336, doi: 10.1046/j.1365-246x.2000.00089.x.

Weaver J.T., Agarwal A.K. and Lilley F.E.M.; 2006: *The relationship between the magnetotelluric tensor invariants and the phase tensor of Caldwell, Bibby, and Brown*. Explor. Geophys., **37**, 261-267, doi: 10.1071/EG06261.

Zezza F., Macri F. and Polemio M.; 1996: *Nuove conoscenze idrogeologiche del Gargano centrale*. Mem. Soc. Geol. Ital., **51**, 1037-1043.

Zunino M., Pavia M., Arzarello M., Bertok C., Di Carlo M., Di Donato V., Graziano R., Matteucci R., Nicosia U., Petronio C., Petrucci M., Pignatti J., Ragusa M., Sacchi E., Sardella R. and Pavia G.; 2012: *Il Gargano, un archivio della diversità geologica dal Mesozoico al Pleistocene*. Giornale di Paleontologia, **4**, 1-139, doi: 10.3301/GFT.2012.02.

Corresponding author: Simona Tripaldi
Dipartimento di Scienze della Terra e Geoambientali, Università degli Studi "Aldo Moro"
Campus Universitario, via Orabona 4, 70125, Bari, Italy
Phone: +39 080 544 2580; e-mail: simona.tripaldi@uniba.it